Dynamics of Light Harvesting in Photosynthesis

Yuan-Chung Cheng and Graham R. Fleming

Department of Chemistry and QB3 Institute, University of California, Berkeley and Physical Bioscience Division, Lawrence Berkeley National Laboratory, Berkeley, California 94720; email: GRFleming@lbl.gov

Annu. Rev. Phys. Chem. 2009. 60:241–62

First published online as a Review in Advance on November 14, 2008

The *Annual Review of Physical Chemistry* is online at physchem.annualreviews.org

This article's doi: 10.1146/annurev.physchem.040808.090259

0066-426X/09/0505-0241$20.00

Key Words

excitation energy transfer, quantum coherence, FMO complex, two-dimensional electronic spectroscopy, pigment-protein complex

Abstract

We review recent theoretical and experimental advances in the elucidation of the dynamics of light harvesting in photosynthesis, focusing on recent theoretical developments in structure-based modeling of electronic excitations in photosynthetic complexes and critically examining theoretical models for excitation energy transfer. We then briefly describe two-dimensional electronic spectroscopy and its application to the study of photosynthetic complexes, in particular the Fenna-Matthews-Olson complex from green sulfur bacteria. This review emphasizes recent experimental observations of long-lasting quantum coherence in photosynthetic systems and the implications of quantum coherence in natural photosynthesis.

1. INTRODUCTION

RC: reaction center

PPC: pigment-protein complex

EET: excitation energy transfer

FMO: Fenna-Matthews-Olson protein of green sulfur bacteria

LHCII: the major light-harvesting complex of plants

Photosynthesis provides chemical energy for almost all life on Earth. The primary event in photosynthesis involves the absorption of sunlight to create electronic excitations in the peripheral antenna of photosynthetic systems and the subsequent transfer of the excitations to a reaction center (RC) (1, 2). An efficient light-harvesting step is critical for the success of photosynthesis, and photosynthetic organisms have evolved sophisticated pigment-protein complexes (PPCs) for this function, with very high yield for light-to-charge conversion (>95%) (2). Rapid excitation energy transfer (EET) from the outer antenna to the RC is required to compete with normal excited-state quenching (3). However, the precise molecular principles that enable such high efficiency have remained elusive because of the lack of both experimental and theoretical tools that can unambiguously reveal couplings and dynamics in complex multicomponent PPCs.

Two fundamental questions regarding the principles of light harvesting can be formulated (1). What are the characteristics of the spatial organization and electronic and electron-nuclear interactions in photosynthetic PPCs that enable effective energy transport (2)? What is the mechanism of EET in light harvesting, and to what extent are quantum mechanical effects involved in this process? Recent advances in structural-based theoretical modeling and emerging spectroscopic tools have provided deeper insight into the interactions and dynamics of photosynthetic systems. In particular, two-dimensional (2D) electronic spectroscopy appears to be well suited for systems such as PPCs because it records couplings and dynamics of energy flow on a 2D map and allows the direct observation of coherence between electronic excitations. We review these recent advances, with a focus on experiments on the Fenna-Matthews-Olson (FMO) protein of green sulfur bacteria.

A full review of the current state of knowledge of the dynamics of light harvesting is impossible. We therefore refer readers to recent reviews covering the peripheral light-harvesting antenna and RC of purple bacteria (4–10), and photosystem I (7, 11) and photosystem II (12) of cyanobacteria and green plants. In particular, van Grondelle & Novoderezhkin (8) present a current review on ultrafast spectroscopy and energy relaxation dynamics in ring-like bacterial antenna complexes and the major light-harvesting complex II (LHCII) of higher plants. Scholes & Fleming (7) also reviewed energy transfer and light harvesting in purple bacterial antenna complexes with a detailed presentation of theoretical descriptions of electronic couplings and EET dynamics. More recently, Sundström (10) reviewed the applications of ultrafast spectroscopy to light-induced biological processes, including the role of carotenoids in light harvesting and photoprotection in photosynthesis.

2. STRUCTURE AND ELECTRONIC EXCITATION IN PHOTOSYNTHETIC COMPLEXES

The availability of high-resolution crystal structures of major photosynthetic complexes has revolutionized our understanding of photosynthetic light harvesting (13). The structural arrangement of pigments and the interactions between the pigments and their protein environment determine the spectral properties and energy transfer characteristics of PPCs. Thus this structural information provides an essential starting point for understanding the design principles of natural light harvesting.

2.1. Structure of Photosynthetic Complexes

The architecture of antenna light-harvesting complexes varies widely among photosynthetic organisms. For example, the antenna complexes of purple bacteria have highly symmetric ring structures, whereas the major light-harvesting complex (LHCII) of higher plants, the most important

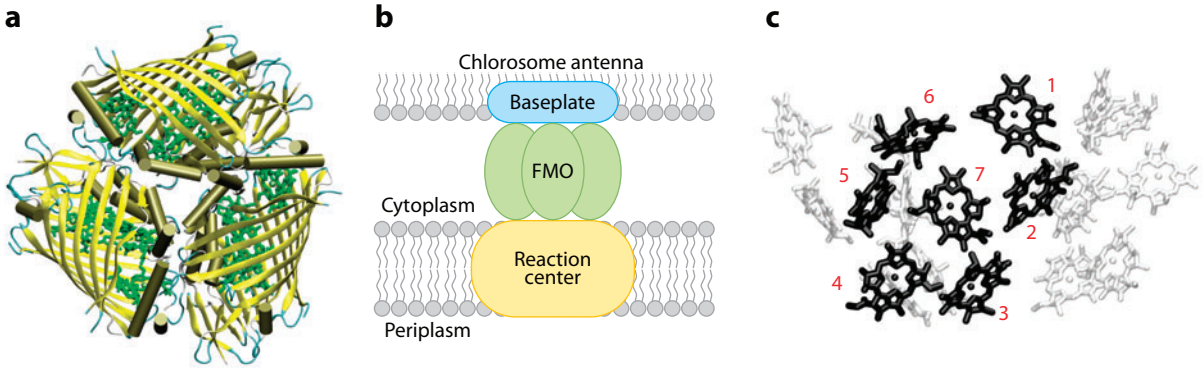

Figure 1

(*a*) Top-view of the Fenna-Matthews-Olson (FMO) protein trimer from green sulfur bacterium *Prosthecochloris aestuarii*. The protein is depicted in yellow, and the bacteriochlorophyll (BChl) molecules are in green. (*b*) The FMO protein is located between the light-harvesting antenna (chlorosome) and the reaction center, with the C3 symmetry axis of the trimer perpendicular to the membrane plane of the baseplate. (*c*) Side view of the BChl arrangement in the FMO trimer. Seven BChl a molecules belonging to one of the monomeric subunits are highlighted in black. The BChl numbers correspond to the original labeling used in Reference 14.

light-harvesting complex on Earth, has a structure with no apparent symmetry. Nevertheless, the structures of photosynthetic complexes share some characteristics that are critical for their functions. A well-studied example is the water-soluble FMO protein of green sulfur bacteria (**Figure 1*a***). Green sulfur bacteria utilize large antenna structures called chlorosomes to harvest sunlight, and the FMO proteins, situated between the chlorosomes and the RC, are responsible for transferring excitation energy from the antenna to the RC (**Figure 1*b***). The FMO complex was the first chlorophyll-protein structure solved by X-ray crystallography with atomic resolution (14). Currently, high-resolution crystal structures of the FMO protein from *Chlorobium tepidum* (15, 16) and *Prosthecochloris aestuarii* (17, 18) are available.

The FMO complex comprises three identical subunits that each contains seven bacteriochlorophyll (BChl) a pigments enclosed in beta sheets. **Figure 1*c*** shows the arrangement of BChls in the FMO trimer. The nearest center-to-center distance between neighboring intrasubunit BChls is ~11 Å, whereas that between intersubunit BChls is ~24 Å. The highly compact packing of BChls facilitated by the protein scaffolding enables strong couplings between BChls and energy tuning via pigment-protein interactions, both of which are important for efficient EET.

2.2. Structure-Based Modeling of Electronic Excitations

The nanoscale dimensions of photosynthetic PPCs produce strong pigment-pigment interactions, resulting in delocalized electronically excited states. Consequently, optical excitations in PPCs are described by the Frenkel exciton model, in which a system made of N chromophores is represented by the Hamiltonian (1, 19)

$$H_e = \sum_{n=1}^{N} \varepsilon_n |n\rangle\langle n| + \sum_{n<m} J_{nm}(|n\rangle\langle m| + |m\rangle\langle n|), \qquad (1)$$

where $|n\rangle$ denotes a molecular excited state at site n, ε_n is the site energy of $|n\rangle$, and J_{nm} is the excitonic coupling between the n-th and m-th chromophores. Diagonalization of H_e gives rise to eigenstates $|\psi_\alpha\rangle$ (exciton states) such that $H_e|\psi_\alpha\rangle = E_\alpha|\psi_\alpha\rangle$. Exciton states in a photosynthetic

BChl: bacteriochlorophyll

PPC are usually delocalized and described as the linear combination of molecular excited states:

$$|\psi_\alpha\rangle = \sum_{n=1}^{N} \phi_n^\alpha |n\rangle. \quad (2)$$

Exciton states form the basis for the description of optical properties and EET dynamics of PPCs. For example, the optical transition dipole moments of exciton states are the linear combination of molecular transition dipoles, $\vec{\mu}_\alpha = \sum_n \phi_n^\alpha \vec{\mu}_n$. As a result, relating the spatial structure of a protein complex to its function (i.e., optical and electronic transfer properties) is a nontrivial task. It requires the determination of the site energies ε_n and electronic couplings J_{nm} to define the exciton states. A model electronic Hamiltonian, however, provides critical insights into the design of PPCs and is indispensable for the interpretation of experimental observations.

2.2.1. Excitonic coupling. The excitonic coupling that gives rise to the EET results from the interactions between the transition dipoles of the chromophores. Conventionally, the excitonic coupling is calculated using a point-dipole approximation as suggested by Förster (20). Convincing evidence has emerged in the past decade that point-dipole approximation is inadequate for this task because of the compact packing of pigments (7, 21). Nevertheless, the excitonic couplings can be obtained straightforwardly based on structural information. For an interpigment distance of >10 Å, the excitonic coupling is determined by the Coulomb interaction between transitions (22–26), which can be calculated exactly using the transition density cube method (24, 25, 27, 28). Based on the same transition density idea, Renger and coworkers (29, 30) recently developed a numerically efficient transition charge from the electrostatic potential method, which has been shown to provide similar accuracy to the transition density cube method.

A critical but less well-explored issue is the influence of the protein environment (21). The protein screens the Coulomb interactions and modifies excited states to alter their transition dipole densities (reaction-field effects). Typically, one uses a screening factor to calculate the effective Coulomb interactions. An effective dipole strength smaller than the solution value for the Q_y transition of BChl is usually required to reproduce experimental observations in PPCs (31), which was explained by the lower electronic polarizability of the protein (29, 30). However, Hsu et al. (32) showed that the polarization of the protein can either decrease or increase the coupling, depending on the orientation and position of the donor and acceptor, indicating that the scaling factor should be used with caution. Recently, Mennucci and coworkers (33, 34) developed a quantum mechanical model that combines a polarizable solvation continuum model and a linear response approach to calculate excitonic couplings in protein environments. This sophisticated treatment reveals a nontrivial distance dependence of excitonic couplings in more than 100 pairs of chromophores taken from photosynthetic complexes (35, 36): The effectiveness of solvent screening decays exponentially as distance decreases in the <20-Å range because of the exclusion of solvent molecules (protein residues) at short interchromophore distances. This is precisely the range of interchromophore distances that is relevant in photosynthesis; therefore, a solvation model with molecular detail seems to be required for the description of EET in photosynthesis.

2.2.2. Energetics of light harvesting. The site energy of an electronic transition is defined as the transition energy of a chromophore from its ground state to an excited state in the absence of electronic coupling with other chromophores. This energy is controlled by the chemical composition of the chromophore and by interactions with the environment. It is difficult to accurately calculate this energy using only structural information because the protein environment as well

as long-range electrostatic interactions play important roles in defining this energy. Furthermore, specific interactions between protein residues and the chromophores can be important (37, 38).

Conventionally, the site energies are obtained by fitting to optical experiments, which becomes unreliable when the number of fitting parameters is large, as in large PPCs with highly congested spectra. In addition, the empirical values do not relate the energy shifts to the molecular details of the PPC, obscuring the mechanisms of energy tuning. Recently, Renger and coworkers (30, 39, 40) calculated the site energies of the seven BChls in a subunit of the FMO complex using only structural information. They treated the BChl Q_y excited state using time-dependent density functional theory and considered a simple electrostatic model that includes the whole protein in atomic detail (39). They showed that the collective electric fields of two α-helices determine the energy shift of the lowest energy site (BChl 3) in the FMO complex and concluded that the main contribution to the site energy tuning arises from electrostatic interactions between the pigments and their surroundings (39, 40). We do not know if these energy-tuning mechanisms are universal, and such detailed modeling of other complexes will be highly informative.

3. THEORETICAL MODELS FOR ENERGY TRANSFER DYNAMICS

In addition to the electronic Hamiltonian, the environment that modulates the electronic excitations and gives rise to relaxation has to be included in a model for EET. The electronic system is coupled to a harmonic bath so that the total system-plus-bath Hamiltonian reads (41)

$$H_{TOT} = H_e + H_B + H_{SB}.$$

A linear system-bath coupling term is usually employed (19, 42):

$$H_{SB} = \sum_n |n\rangle\langle n| \cdot q_n, \tag{3}$$

where q_n is a collective bath coordinate coupled to the n-th chromophore. It is generally assumed that the bath modes modulating different chromophores are uncorrelated, so that $\langle q_n(t)q_m(0)\rangle = 0$ when $n \neq m$. This form of H_{SB} represents independent phonon-induced fluctuations of the site energies on each chromophore. Within this model, the details of the bath are not important, and the dynamics is related to the spectral density, $J_n(\omega)$, which represents the coupling strength and density of states of the phonon bath. In principle, the spectral density can be obtained from ultrafast nonlinear spectroscopic techniques (43). The strength of system-bath coupling is measured by the bath reorganization energy $\lambda_n = \int_0^\infty d\omega J_n(\omega)/\omega$.

This microscopic model provides a consistent means to calculate various linear and nonlinear spectra of the system, as well as the EET dynamics through a perturbative treatment (19, 44). Two limits of EET dynamics can be identified: When the electronic coupling (J_{nm}) is small, a localized description of the donor and acceptor excited states is an appropriate representation, and a perturbation theory treatment of excitonic couplings gives rise to the Förster picture of EET dynamics. Conversely, when the system-bath coupling is weak (i.e., $\lambda \ll J$), a delocalized excitonic representation is needed, and a perturbation theory treatment of H_{SB} yields the Redfield equations. We discuss these limits of EET dynamics in the following section.

3.1. Weak Electronic Coupling Limit: Förster Theory and Multichromophoric Effects

The classic Förster theory of EET assumes incoherent hopping between chromophores induced by point dipole–point dipole interaction between chromophore transition dipoles (21). The simple

Förster equation is inadequate in photosynthetic systems because the nanoscale packing of the pigments results in the breakdown of the point-dipole approximation and, more importantly, because the coherence within donor or acceptor subunits can modify the spectral properties of chromophores and electronic interactions between them (21). A key insight recognized by Scholes and coworkers (45, 46) and independently by Sumi (47, 48) is that EET between blocks of excitonically coupled molecules proceeds via delocalized exciton states, not the molecular units. Silbey and coworkers (49, 50) later formulated a multichromophoric generalization of the Förster theory that gives the idea a firm theoretical footing. Their multichromophoric Förster resonance energy transfer theory treats nonequilibrium effects (50) and has been extended to treat correlated fluctuations between donor and acceptor modes (51). This model considers excitations delocalized over a small group of molecules and a picture of hopping between these groups, which seems to provide a satisfactory description for the motion of excitations in energetically well-separated components, such as the antenna of purple bacteria (5, 52, 53). However, multichromophoric Förster resonance energy transfer theory alone cannot provide a complete description of EET in a PPC because EET within strongly coupled donor (or acceptor) groups still requires a coherent description of dynamics.

3.2. Weak System-Bath Coupling: Redfield Dynamics

When the electronic coupling is strong and the system-bath coupling is weak, it is necessary to consider relaxation between delocalized exciton states. In this limit, the EET dynamics are described by the coupled Redfield equations in the exciton basis (41, 54):

$$\frac{d}{dt}\rho_{\alpha\beta}(t) = -i\omega_{\alpha\beta}\rho_{\alpha\beta}(t) - \sum_{\gamma\delta} R_{\alpha\beta,\gamma\delta}(t)\rho_{\gamma\delta}(t), \tag{4}$$

where $\omega_{\alpha\beta} = E_\beta - E_\alpha$ is the energy gap between excitons. The first term in Equation 4 describes coherent evolution governed by H_e (Equation 1). The second term corresponds to bath-induced dissipative dynamics. The Redfield tensor element $R_{\alpha\beta,\gamma\delta}(t)$ describes the transfer rate from $\rho_{\gamma\delta}$ to $\rho_{\alpha\beta}$ at time t. A second-order perturbation treatment based on H_{SB} (Equation 3) yields the tensor elements in terms of correlation functions:

$$\begin{aligned} R_{\alpha\beta,\gamma\delta}(t) = -\int_0^t d\tau \Bigg[& \langle V_{\delta\beta}(0)V_{\alpha\gamma}(\tau)\rangle e^{-i\omega_{\delta\beta}\tau} + \langle V_{\delta\beta}(\tau)V_{\alpha\gamma}(0)\rangle e^{-i\omega_{\alpha\gamma}\tau} \\ & - \delta_{\delta\beta}\sum_s \langle V_{\alpha s}(\tau)V_{s\gamma}(0)\rangle e^{-i\omega_{s\gamma}\tau} - \delta_{\gamma\alpha}\sum_s \langle V_{\delta s}(0)V_{s\beta}(\tau)\rangle e^{-i\omega_{\delta s}\tau} \Bigg], \end{aligned} \tag{5}$$

where, according to Equations 2 and 3,

$$\langle V_{\delta\beta}(0)V_{\alpha\gamma}(\tau)\rangle = \sum_n \phi_n^\alpha \phi_n^\beta \phi_n^\gamma \phi_n^\delta \cdot \langle q_n(0)q_n(\tau)\rangle. \tag{6}$$

In general, $R_{\alpha\beta,\gamma\delta}(t)$ is time dependent; however, when the timescale of interest is long compared with the bath relaxation time τ_b (55, 56), the Markovian approximation can be applied using $R_{\alpha\beta,\gamma\delta}(t = \infty)$. The Redfield equations given in Equations 4 and 5 describe the full dynamics of the system, including (*a*) $R_{\alpha\alpha,\beta\beta}$, population transfer from $|\beta\rangle$ to $|\alpha\rangle$; (*b*) $R_{\alpha\beta,\alpha\beta}$ ($\alpha \neq \beta$), dephasing of the $|\alpha\rangle\langle\beta|$ coherence; and (*c*) $R_{\alpha\beta,\gamma\delta}$ ($\omega_{\alpha\beta} - \omega_{\gamma\delta} \neq 0$), coherence transfer from $|\gamma\rangle\langle\delta|$ to $|\alpha\rangle\langle\beta|$. We note that the correlation functions in Equation 6 are determined by the spatial overlap of the exciton wave functions and bath correlation functions (57). Thus, Redfield theory predicts rapid energy transfer between exciton states that have strong overlap of their wave functions.

The contribution from the Redfield tensor element $R_{\alpha\beta,\gamma\delta}$ is calculated by integrating over an integrand that oscillates at a frequency $\Delta\omega = |\omega_{\alpha\beta} - \omega_{\gamma\delta}|$, and thus the contribution averages out on a timescale of $\Delta\omega^{-1}$. Consequently, the population transfer ($R_{\alpha\alpha,\beta\beta}$) and dephasing ($R_{\alpha\beta,\alpha\beta}$) terms are more effective in the relaxation process because $\Delta\omega = 0$. This is the basis of the popular secular approximation (54), in which the coherence transfer terms with $\Delta\omega \neq 0$ are assumed to be negligible. However, a nonsecular term can have significant contribution when (*a*) the oscillating frequencies of the two coherences ($\omega_{\alpha\beta}$ and $\omega_{\gamma\delta}$) are close to each other, so that $\Delta\omega$ is small and $\Delta\omega^{-1}$ is longer than the timescale of interest (58), and (*b*) when the exciton states are delocalized, so that the cross correlation of bath-induced energy fluctuations is significant (Equation 6) (59). A photosynthetic complex with strong excitonic coupling and dense, almost equally spaced exciton levels satisfies these criteria. Ultrafast fluorescence anisotropy studies on the LH2 antenna complex indicate that the full Redfield treatment is necessary to reproduce the long-lived coherences and higher anisotropy values observed in the experiments at <2 ps (60, 61). A recent 2D experiment on the FMO complex also indicates that coherence transfer can play a role in light-harvesting EET (62). It is well established in vibrational relaxation that these nonsecular coherence transfer terms can actually contribute to the nuclear wave-packet dynamics (63, 64). However, in electronic EET dynamics, the effect of these coherence transfer terms has not been systematically studied in the literature.

LH2: the LH2 antenna complex of purple bacteria

Redfield theory assumes that the electron-phonon coupling is weak and that the spectrum of the phonon bath is broad (compared to the energy gap between exciton states) so that only single-phonon processes are required. Yang & Fleming (42) examined the limitations of the Redfield formalism and concluded that the later point is more stringent and limits the applicability. In other words, Redfield theory breaks down when multiphonon processes are important, which is likely to be the case for large energy gaps or low temperatures.

3.3. Intermediate Coupling Regime

Modeling EET dynamics in the intermediate coupling regime, in which the electronic coupling is comparable to the bath organization energy, is a challenging problem. This is evident in treatments of exciton migration in molecular crystals (65–67). It is becoming clear that in many photosynthetic systems, a small parameter does not exist, and a theory applicable to the intermediate coupling regime is required (8, 68–71). First suggested by Zhang et al. (72) and further explored by Yang & Fleming (42), the modified-Redfield approach treats diagonal bath reorganization in the exciton basis exactly and the off-diagonal fluctuations using second-order perturbation theory. Because multiphonon reorganization effects are treated exactly, the modified-Redfield approach gives reasonable results when conventional Redfield equations break down (42). Consequently, the modified-Redfield approach has gained popularity. For example, van Grondelle and coworkers showed that the modified-Redfield approach provided a significantly better description for EET dynamics in LH2 (69) and LHCII (68). Renger et al. (71) found that modified-Redfield theory yields a better prediction for the downhill population transfer rate in a Chl a/Chl b heterodimer in the water-soluble chlorophyll binding protein and concluded that modified-Redfield theory needs to be used if the energy gap between the exciton states is larger than approximately 200 cm^{-1}. However, the modified-Redfield approach is based on a diagonal projection operator approach, and therefore, unlike the full Redfield approach, it does not describe coherence dynamics. This limits its applications to population dynamics in the exciton basis. The pure dephasing reference system approach developed by Golosov & Reichman (73, 74) adopts a similar framework and treats the full coherence dynamics. However, applying their approach to treat EET dynamics in PPCs appears to be a formidable task because of the highly complicated inhomogeneous terms in its equations.

Issues such as dynamical localization effects, coherence transfer dynamics, and more general forms of system-bath couplings are largely overlooked in present models of light-harvesting EET dynamics. For example, almost all existing theories assume independent fluctuations of energies at different sites; however, recent experiments (62, 75) suggest that correlated energetic fluctuations and bath modulation of the electronic couplings might be important in photosynthetic PPCs (52). In summary, a complete and practical theoretical description of full coherent EET dynamics in the intermediate coupling regime is not yet available.

4. TWO-DIMENSIONAL ELECTRONIC SPECTROSCOPY

Excitation energy transfer in photosynthetic systems often occurs on a subpicosecond timescale, making ultrafast spectroscopic methods indispensable for probing EET dynamics (8, 10). The difficulty of directly probing electronic couplings and of resolving dynamics in optically congested multichromophoric systems makes it extremely challenging to obtain detailed dynamical information. However, the advent of 2D electronic spectroscopy, a new type of photon echo measurement, has changed this situation. In this section, we briefly review the principles of 2D electronic spectroscopy and the applications of the 2D technique to the study of photosynthetic systems and refer the reader to several recent surveys of the theoretical underpinning (76–78), experimental setup (77), and other applications (78, 79) of 2D electronic spectroscopy.

A 2D experiment utilizes three laser pulses to interrogate the sample and uses heterodyne detection for the signal field in the phase-matching direction $k_s = -k_1 + k_2 + k_3$. Fourier transformation with respect to the time delay between the first and second pulses (coherence time, τ) and the time delay between the third pulse and signal (rephasing time, t) yields the frequency domain 2D electronic spectrum at a fixed time delay between the second and third pulses (population time, T). **Figure 2*a*** shows a model 2D spectrum for a three-component system (80). In contrast to

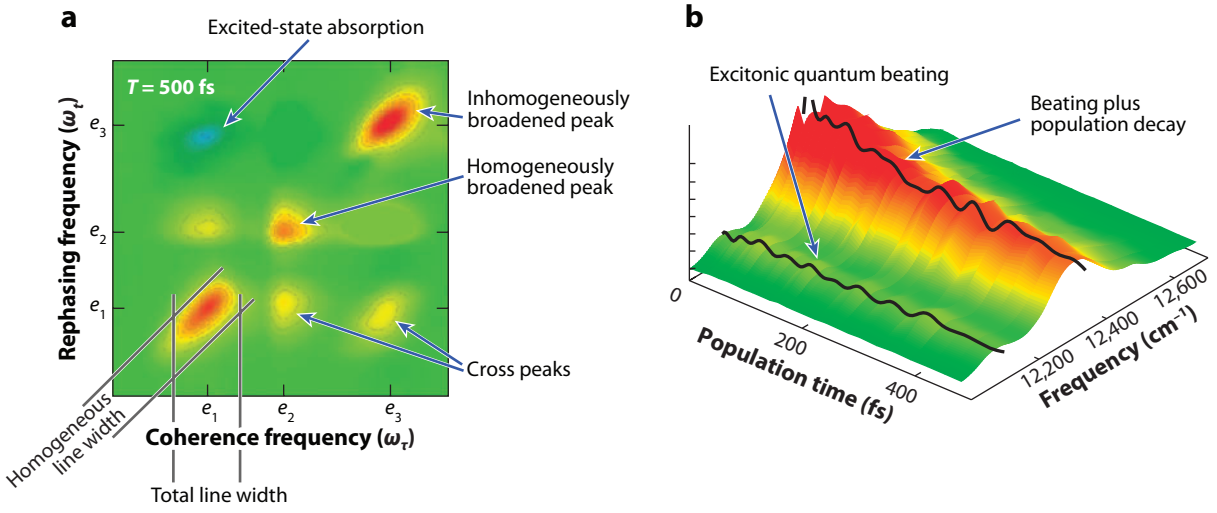

Figure 2

Information content in 2D spectra. (*a*) Model 2D spectrum for a three-component system (e_1, e_2, and e_3). The 2D spectrum can be viewed as a map that correlates the absorption (ω_τ) and emission (ω_t) frequencies of the system. (*b*) Time evolution of the diagonal slice of the 2D spectrum of the *Chlorobium tepidum* Fenna-Matthews-Olson complex (62). The 2D technique is most informative when spectra measured at different population times are connected to visualize the dynamics of spectral features. For example, the black lines emphasize the excitonic coherence dynamics in the amplitude beating of the exciton 1 peak and the additional population relaxation dynamics in the decay of the exciton 3 peak.

vibrational 2D spectra, electronic 2D spectra of excitonic systems show no symmetry around the diagonal. The geometry of the complex determines how the oscillator strength is redistributed between the various ground to one-exciton and one- to two-exciton transitions (79).

The 2D spectrum (**Figure 2*a***) provides a map that correlates frequencies of the system between the initial (τ) and final (t) time intervals. Excitation and the subsequent emission from the same transition give rise to a diagonal peak ($\omega_\tau = \omega_t$), showing the energy level of the exciton. Energy fluctuations induced by system-bath coupling result in a symmetric, homogeneously broadened peak (at large T) because the dynamical processes rapidly scramble the energy of the exciton. In contrast, when a system has a wide distribution of transition energies due to different environments, each exciton keeps the same transition frequency during the duration of the experiment. This correlation leads to an elongation of the peak along the diagonal, showing an inhomogeneously broadened peak (**Figure 2*a***). Thus, the transient behavior of a 2D lineshape reveals solvation dynamics and solute-solvent interactions (81–83). Cross peaks at $T = 0$ arise because the same molecule, or molecules, contributes to, for example, two different transitions in the absorption spectrum. In other words, they reveal delocalized excitations and electronic couplings in the system (84, 85). At longer population times, cross peaks appear through energy transfer. We plot the spectrum such that these cross peaks appear below the diagonal. For example, the two cross peaks in **Figure 2*a*** show that energy transfer from $e_3 \rightarrow e_1$ and $e_2 \rightarrow e_1$ occurs on the 500-fs timescale. Such correlations allow an unambiguous assignment of parallel pathways, which makes the 2D technique a particularly powerful tool for monitoring EET dynamics in networks of coupled chromophores (57, 80, 84).

Moreover, because 2D electronic spectroscopy records the signal at the level of the field rather than the intensity, it is sensitive to the quantum phase evolution of the system. A broadband pulse interacts with all excitons and can produce superpositions (coherences) of exciton states. **Figure 3**

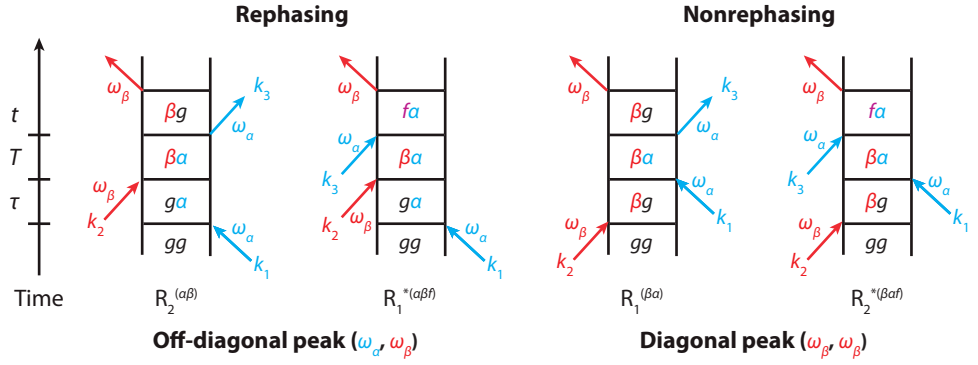

Figure 3

Impulsive limit double-sided Feynman diagrams representing contributions to the 2D signals from the coherence pathways. These diagrams describe the evolution of density matrix elements, where g denotes the ground state, the Greek letters denote one-exciton states, and f represents a two-exciton state. The time axis goes from bottom to top, and the arrows represent system-field interactions, in which the three laser pulses in a 2D experiment are labeled by k_1, k_2, and k_3. For these pathways, the system is prepared in a coherence state $|\beta\rangle\langle\alpha|$ during the population time delay; therefore, an oscillating phase factor with a frequency of $\omega_{\alpha\beta}$ is associated with all these terms. These diagrams can be divided into the rephasing and the nonrephasing contributions. In rephasing contributions (*left*), the system evolves in conjugate frequencies during τ and t, which gives rise to a photon echo signal. In nonrephasing contributions (*right*), the phase factors associated with the evolution of coherences during τ and t have the same sign, resulting in free induction decay during t. Here we show that coherence pathways contribute to cross peaks in rephasing spectra; however, in nonrephasing spectra, the coherence pathways contribute to diagonal peaks.

shows double-sided Feynman diagrams representing contributions from such coherence pathways. These diagrams describe the evolution of density matrix elements: The first two pulses interact with two different exciton states (denoted $|\alpha\rangle$ and $|\beta\rangle$) to prepare a coherence $|\beta\rangle\langle\alpha|$ during the population time T, and the third pulse then interacts again with $|\alpha\rangle$ to induce a signal. The time evolution of the $|\beta\rangle\langle\alpha|$ coherence during T has an oscillating phase factor with a frequency $\omega_{\alpha\beta}$ (Equation 4), resulting in quantum beats in the 2D spectra that can be related quantitatively to the coherence dynamics of the system (80, 84–86). Such quantum beats were observed in 2D electronic spectra of the *C. tepidum* FMO complex (**Figure 2*b***) (62). In addition, the rephasing ($\tau > 0$) and nonrephasing ($\tau < 0$) coherence contributions give rise to beating on the cross peaks and on the diagonal peaks, respectively (**Figure 3**) (64, 86–88).

Linear absorption and conventional pump-probe spectroscopy are insensitive to the nature of electronic couplings, whereas 2D spectroscopy provides a direct probe for interactions and dynamics even in overlapping optical bands. For example, in the purple bacterial light harvesting complex LH3 (89), the 2D spectra clearly show that EET to dark states dominates B800 to B820 energy transfer (89), as had been predicted earlier by theory (24, 45). Furthermore, the B800 diagonal peak shows pronounced asymmetry around the diagonal even for weak electronic couplings ($\sim$30 cm^{-1}) and substantial static energetic disorder ($\sim$80 cm^{-1}) (89). If the B800 molecules were completely uncoupled, the diagonal peak corresponding to the B800 band would be symmetric about the diagonal. This experiment demonstrated the exquisite sensitivity of the 2D lineshape to weak couplings. Through the redistribution of oscillator strength in the one- to two-exciton manifold and the subsequent interference between the diagonal peak (positive) and off-diagonal excited-state absorption contributions (negative), real 2D lineshape reports electronic coupling even when no cross peak is visible.

The 2D spectra of light-harvesting PPCs generally contain many overlapping bands that complicate the interpretation. Thus developing variants of 2D electronic spectroscopy for enhanced specificity and resolution is currently an active field of research. First suggested by Hochstrasser (90) and Zanni et al. (91) and later explored by Dreyer et al. (92), the polarization of laser pulses can be rotated to manipulate the relative contributions of Liouville pathways to enhance or suppress specific spectral features. For example, by using a cross-peak specific polarization sequence $(\pi/3, -\pi/3, 0, 0)$, Read et al. (93) showed that cross peaks can be isolated from the stronger diagonal peaks in the 2D spectrum of the FMO complex from *Pelodictyon phaeum*. Mukamel and coworkers (94) have taken a further step and proposed using polarization pulse shaping to suppress diagonal peaks and amplify cross peaks based on the complex chirality and fundamental symmetries of multidimensional optical signals (95–97). These extensions to 2D electronic spectroscopy take advantage of the relative orientations of excitonic transitions and can provide powerful tools to pick apart spectral signatures in a congested 2D spectrum to probe specific dynamics of interest, much like the programming of pulse sequences in multidimensional nuclear magnetic resonance. Read et al. (98) showed that nonrephasing spectra yield important information not apparent in the rephasing or total correlation spectra and are especially powerful when combined with varying polarization conditions.

5. DYNAMICS OF ENERGY TRANSFER IN THE FMO COMPLEX

The FMO complex represents an important model in photosynthesis because of its relatively small size and lack of symmetry. In addition to structural data, theoretical studies (30, 31, 57, 99–101) and ultrafast spectroscopic experiments (62, 102–104) have paved the way to a detailed understanding of this system. Here we review recent measurements on the FMO complex obtained via 2D electronic spectroscopy. These results generally corroborate previous studies and

provide unprecedented details about the electronic structure and dynamics of energy transfer in FMO.

5.1. Excitonic Structure of the FMO Complex

The development of a general method to measure excitonic coupling in photosynthetic complexes is a challenging task. Methods based on two-color three-pulse photon echo peak shift measurements have been successful for spectrally well-resolved systems (105–108); however, for most PPCs, the spectrum is highly congested, and the two-color selectivity is unattainable. Read et al. (98) took polarization-dependent 2D electronic spectra of the FMO complex from *P. aestuarii* using three-pulse polarization conditions: ⟨0°, 0°, 0°, 0°⟩, ⟨45°, −45°, 0°, 0°⟩, and ⟨75°, −75°, 0°, 0°⟩ (**Figure 4**). The polarization-dependent 2D nonrephasing spectra are sensitive to the relative orientations between transition dipoles of excitons, which are determined by the pigment arrangement and the redistribution of transition dipoles owing to electronic couplings. Spectra taken at different polarization conditions together provide a stringent test of a model electronic Hamiltonian. The model Hamiltonian proposed by Renger and coworkers (30, 39) based solely on structural information provides a semiquantitative description of the measurements (98).

Furthermore, Read et al. (98) focused on nonrephasing spectra and the cross peak produced by energy transfer from exciton 4 to exciton 2 (**Figure 4*c***). The amplitude of this peak depends on the polarization conditions. In the ⟨45°, −45°, 0°, 0°⟩ spectrum, the peak is suppressed, whereas it is enhanced in the ⟨75°, −75°, 0°, 0°⟩ spectrum. Model calculations showed that the amplitude variation is only reproduced when the angle between the two transition dipoles is ∼40°. This observation cannot be explained by the orientations of the transition dipole moments of the localized molecular excitations and requires redistribution of transition dipole moments due to delocalization of the exciton states (**Figure 4*b***). In other words, this technique enables visualization of the relative orientations of the excitons. If the structure is known, the excitonic transition dipole moments are determined by wave functions of the excitons, which is directly related to the electronic Hamiltonian (Equations 1 and 2). The result indicates that the combination of 2D nonrephasing and polarization techniques enables a direct probe for the coarse-grained information about the relative orientations of the excitonic transition dipoles and a direct link to the electronic landscape.

5.2. Energy Transfer Pathways

The excitonic couplings and site energies of excited states in the FMO complex have been used to describe the dynamics of excitation transfer (30, 31, 57, 99–101). Brixner et al. (104) studied EET in the FMO complex from *C. tepidum* using the 2D technique. They took 2D spectra at several population time points, providing snapshots of excitation motion within the FMO complex. **Figure 5*a*** shows the 2D spectrum at $T = 0$ fs. The cross peaks below the diagonal reveal electronic couplings between excitonic states. The data were combined with theoretical modeling to demonstrate that the energy flow within the FMO complex occurs primarily through two energy transfer pathways (**Figure 5*b***) (57, 104), which connect spatially proximate and excitonically coupled dimers. Cho et al. (57) presented a detailed theoretical analysis of the experimental data and suggested that population dynamics in the FMO complex can be described by a combination of Förster theory and modified-Redfield equations.

Brixner et al. (104) showed that although the two pathways affect an overall funneling of the energy from higher-energy sites to the lowest-energy trap, the energy transport is not a simple

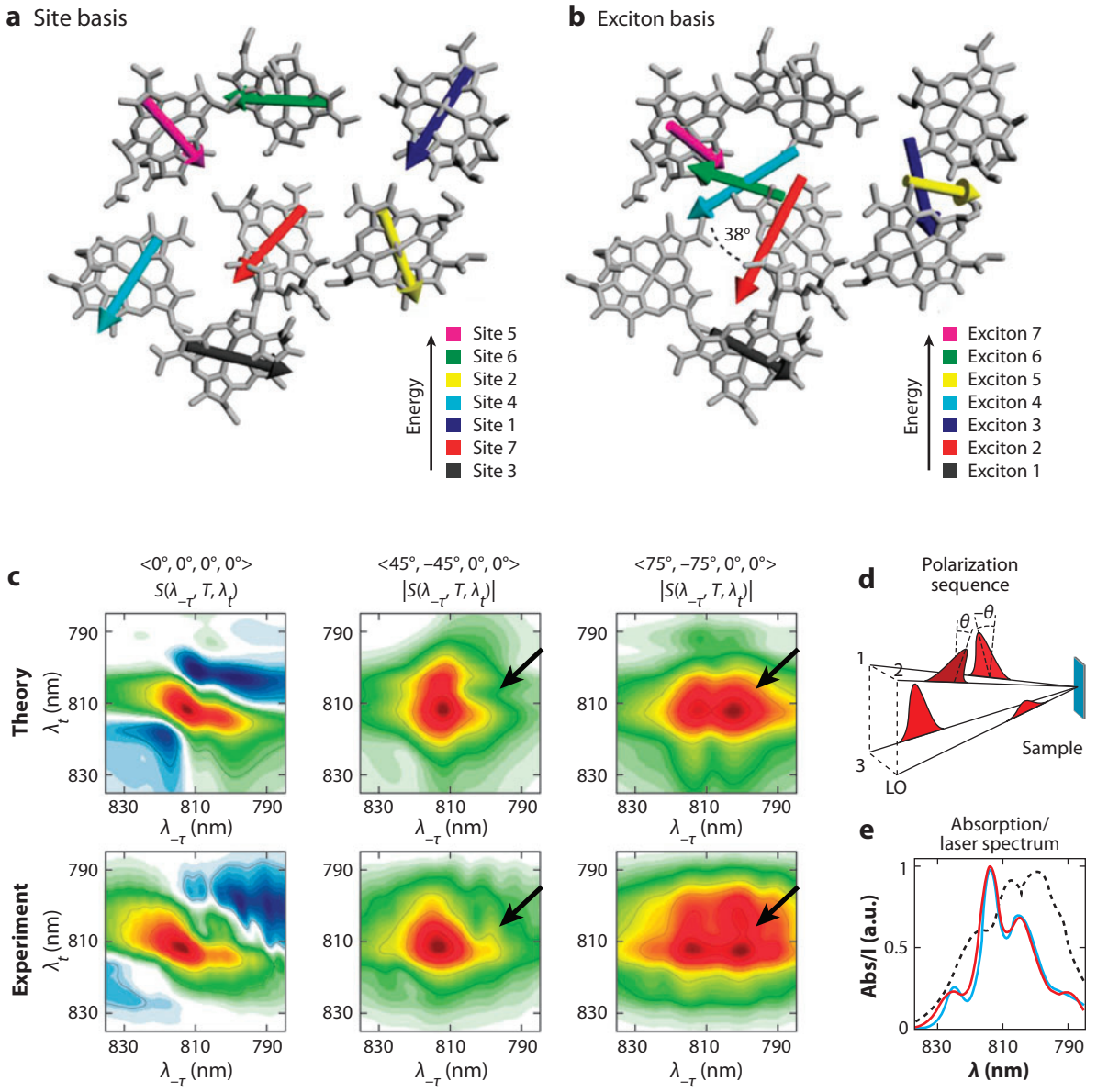

Figure 4

Orientations of Q_y transitions of the seven bacteriochlorophyll (BChl) molecules in the Fenna-Matthews-Olson (FMO) protein from *Prosthecochloris aestuarii* (98). The molecular transition dipole moments shown in the site basis (*a*) are redistributed among excitons owing to electronic couplings between BChls, resulting in different positions and orientations of the excitonic transition dipoles in the exciton basis (*b*). The dominant features in the short-time 2D spectra arise from excitons 2 and 4, whose transition dipoles are shown in red and cyan, respectively. (*c*) Theoretical and experimental nonrephasing spectra of the FMO complex measured at $T = 400$ fs and 77 K using polarization conditions $\langle 0°, 0°, 0°, 0° \rangle$, $\langle 45°, -45°, 0°, 0° \rangle$, and $\langle 75°, -75°, 0°, 0° \rangle$. The black arrows indicate the exciton 4 to exciton 2 energy transfer cross peak that is suppressed in the $\langle 45°, -45°, 0°, 0° \rangle$ spectrum and enhanced in the $\langle 75°, -75°, 0°, 0° \rangle$ spectrum. (*d*) The polarization-dependent 2D pulse sequence. (*e*) The experimental and theoretical linear absorption spectra are shown in cyan and red, respectively, and the dotted line is the laser pulse profile. Figure reprinted with permission by *Biophysical Journal*; figure originally appeared in E.L. Read, G.S. Schlau-Cohen, G.S. Engel, J. Wen, R.E. Blankenship & G.R. Fleming, *Biophys. J.* 95:847–56 (July 2008).

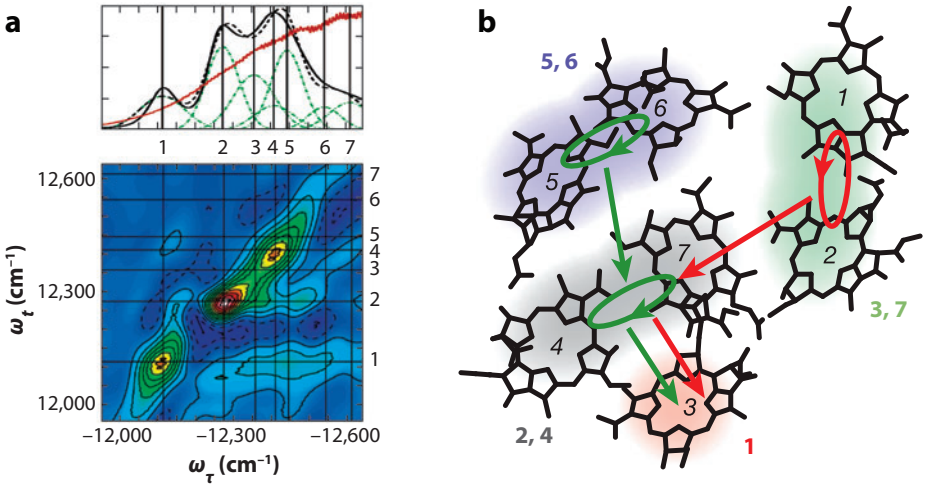

Figure 5

Exciton delocalization and energy flow in the Fenna-Matthews-Olson (FMO) complex (104). (*a*) The linear absorption and $T = 0$ fs 2D spectrum of the *Chlorobium tepidum* FMO complex. Individual exciton bands are shown in green, and the red curve indicates the laser spectrum in the experiment. (*b*) The FMO structural arrangement of the seven bacteriochlorophyll molecules (*italic numbers*) overlaid qualitatively with the delocalization patterns of the excitons (*colored shading*, *bold numbers*). Two main excitation energy transfer pathways are indicated by the red and green arrows. Figure reprinted by permission from Macmillan Publishers Ltd: *Nature*; figure originally appeared in T. Brixner, J. Stenger, H.M. Vaswani, M. Cho, R.E. Blankenship & G.R. Fleming, *Nature*, 434:625–28 (2005); copyright 2005.

process of stepwise energy decrease from one exciton level to the next lowest level. Instead, it depends sensitively on detailed spatial properties of the excited-state wave functions, as predicted by Redfield theory. In addition, BChl 3 was also identified as the energy trap within the FMO, which is consistent with recent theoretical calculations (30, 31, 57, 99, 101). The result suggests that the FMO complex is organized so that BChls 3 and 4 are in contact with the RC, which has been recently confirmed by Blankenship and coworkers (109). The combined spatial and energetic landscape of the complex enables the excitation to move to the lowest energy state in two or at most three steps, no matter where the excitation starts. This overall picture of EET in light harvesting is notably different from a random diffusion model that has been considered previously (110, 111).

5.3. Mechanism of Energy Transfer

That chromophores in photosynthetic PPCs produce delocalized states has been evident for some time (112–115), but techniques to reveal whether quantum coherence effects were relevant to their function were lacking. Hints of quantum coherence in photosynthetic complexes have been observed using pump-probe anisotropy techniques (60, 61, 116); however, it was difficult to unambiguously assign these observations to an electronic origin. Indeed, it is generally assumed that electronic coherence decays so rapidly that it does not affect the EET.

Two-dimensional electronic spectroscopy provides a unique probe that is sensitive to the coherent phase evolution of quantum systems. Recently, Engel et al. (62) investigated the FMO complex of *C. tepidum* and took multiple 2D spectra from $T = 0$ to $T = 660$ fs at 77 K. The evolution of the diagonal slice of the 2D spectrum reveals a complex quantum beating pattern

that is entirely explainable in terms of the exciton levels of the system (**Figure 6**). **Figure 6*d*** shows the anticorrelation between the amplitude of the exciton 1 diagonal peak and the ratio of the diagonal to antidiagonal widths of the peak, which is a characteristic predicted from theory for exciton quantum beating (84, 86). The observed quantum beats clearly lasted for timescales similar to the EET timescales (**Figure 6*d***), showing that excitations move coherently through the

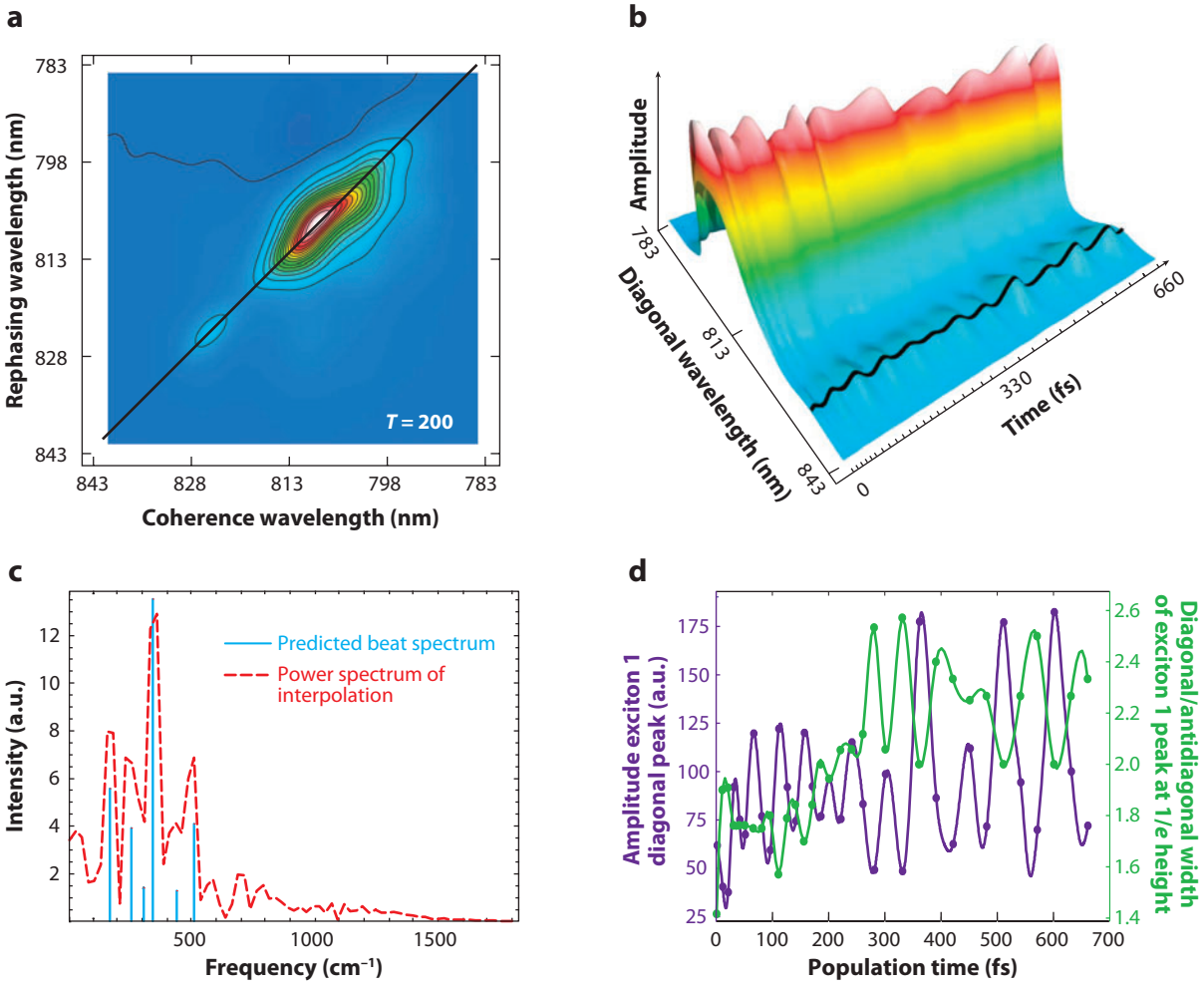

Figure 6

Coherence quantum beating in the Fenna-Matthews-Olson (FMO) complex (62). (*a*) The 2D spectrum of the FMO complex measured at $T = 200$ fs and 77 K. (*b*) Time evolution of the diagonal slice of the 2D spectrum. The beating signal of the first exciton peak is emphasized with the solid black line. (*c*) Comparison between the interpolated power spectrum of this first exciton beating signal (*dashed curve*) and the theoretical beat spectrum predicted by the excitonic energy structure (*cyan stick spectrum*). The excellent agreement indicates that the observed beating signal represents long-lasting electronic quantum coherence in the system. A similar analysis can be made for the other exciton peaks in the 2D spectrum. (*d*) The amplitude of the exciton 1 diagonal peak (*purple curve*) and the ratio of the diagonal to antidiagonal widths of the peak (*green curve*). The anticorrelation is a characteristic of excitonic quantum beating (84, 86). This pattern would not arise from phonon coupling and highlights the interplay between the rephasing and nonrephasing contributions in 2D spectra. Figure reprinted by permission from Macmillan Publishers Ltd: *Nature*; figure originally appeared in G.S. Engel, T.R. Calhoun, E.L. Read, T.K. Ahn, T. Mančal, Y.-C. Chung, R.E. Blankenship & G.R. Fleming, *Nature*, 446:782–86 (2007); copyright 2007.

FMO complex, rather than by incoherent hopping as had usually been assumed (110). In addition, the beating amplitude of the cross peak between exciton 1 and 3, which traces the amplitude of the coherence between the two excitons (80), is minimum at $T = 0$ and increases as a function of T. This indicates that coherence is transferred into the 1–3 coherence. According to the discussion in Section 3.2, such a coherence transfer effect requires an energy-matching condition and correlated bath fluctuations (58, 59, 63, 64, 117); therefore, a more general theoretical model that includes a correlated nonlocal bath, coherence transfer dynamics, and non-Markovian dynamics will be required to describe the observations. We note that the beating on the diagonal in **Figure 6** arises solely from the nonrephasing contribution and therefore provides another example of the utility of recording the separate rephasing and nonphasing spectra. Nonrephasing spectra provide a precise way to determine beat frequencies and dephasing times, as recently demonstrated by Calhoun et al. (118).

The observation of long-lasting quantum coherence also led to the suggestion that quantum effects might be utilized in the FMO complex to promote light harvesting. Engel et al. (62) proposed that the FMO complex performs a quantum search algorithm that is more efficient than a classical random walk suggested by the hopping mechanism. Quantum coherence enables the excitation to rapidly and reversibly sample multiple pathways to search for the site (BChl 3) that connects to the RC (119). A second advantage of the reversible motion is that it is more difficult to become trapped in a subsidiary energy minimum. Further studies are required before it can be stated that quantum coherence is a general feature of photosynthetic PPCs, but it seems clear that any accurate description of the dynamics (and design principles) of these systems will require proper consideration of this true quantum effect.

The long-lasting quantum coherence revealed in the FMO complex is not unique. In an independent study using a different method that is specifically sensitive to coherences, the two-color electronic coherence photon echo technique, Fleming and coworkers (75) directly observed coherence dynamics in a photosynthetic bacterial RC and revealed a long-lasting electronic coherence between two electronic states that are formed by mixing of the bacteriopheophythin and accessory BChl excited states. This experiment yielded Gaussian dephasing times of 440 and 310 fs at 77 and 180 K, respectively. Furthermore, the long-lasting coherence can be explained only by strong correlations between protein motions that modulate electronic transition energies of neighboring chromophores. The combined results of References 62 and 75 suggest that correlated protein environments preserve electronic coherence in photosynthetic complexes and contribute to the optimization of photosynthetic EET.

6. WHAT DOES QUANTUM COHERENCE HAVE TO DO WITH NATURAL LIGHT HARVESTING?

Do these observations made using coherent laser excitation represent the reality of natural light harvesting? A frequent concern is that the coherence is created only by the ultrashort laser pulses used in the experiments, and the sun, being an incoherent light source, would not produce the same effect. It is certainly true that by synchronizing the entire ensemble, the femtosecond laser pulses enable us to observe the quantum aspects of the system, but the function of light harvesting does not depend on such ensemble coherence. Phase coherence within an individual complex would allow quantum coherence to affect the dynamics of EET. The sun is a source of broadband black-body radiation that can be viewed as a series of random ultrashort spikes with a duration as short as the bandwidth allows (120–122). At the single system level, excitation by sunlight also generates a coherent superposition of excited states. Preparation by energy transfer from another light-harvesting complex can also produce delocalized superposition states, and phonon-induced

coherence transfer dynamics can induce excitonic coherence after the transfer (63, 117). Generally speaking, in natural light harvesting, coherence at an individual system level can be generated, and the quantum effect can affect the outcome of energy trapping, as long as the coherence within a single system is maintained. If a dozen quantum computers each independently executed a quantum algorithm, for example, no one would imagine that 12 computers should be started at the same instant for each to arrive independently at the correct result.

The mechanisms responsible for long-lasting coherence observed by coherent laser experiments are also relevant in natural light harvesting. These experiments are carried out with weak light pulses whose electronic fields do not alter the Hamiltonian of the complex. The terms in the Hamiltonian that give rise to the long-lasting coherence observed are intrinsic. The key characteristic of the photosynthetic complexes is the small reorganization energy, λ (7). With the spin-boson model, one can estimate a lower bound for the Gaussian dephasing time as a function of temperature and λ in the high-temperature limit using (43, 123)

$$\frac{1}{\tau_g} = \sqrt{2\lambda k_b T}.$$

For $\lambda = 80\ \mathrm{cm}^{-1}$, which is a typical value measured for chlorophyll Q_y excitation in photosynthetic complexes, $\tau_g = \sim$60 fs at 77 K and $\tau_g \sim 30$ fs at 298 K. Additionally, if we consider that not all the reorganization energy may be expressed on the timescale of very rapid energy transfer and that correlated protein environments and phonon-induced coherence transfer processes can further extend dephasing times (75), it is plausible that the long-lasting coherence observed in complex photosynthetic PPCs could play a role in light harvesting.

7. CONCLUDING COMMENTS

The efficiency of light harvesting and hence photosynthesis is controlled by the competition between loss through radiative and nonradiative decay and trapping at the reaction center; thus the rapid EET on a subpicosecond timescale is crucially important to the success of photosynthesis. Theoretical studies based on high-resolution structures have shown that the nanoscale dimensions in photosynthetic PPCs are responsible for their effective function. This leads to strong couplings between molecular excitations and provides a means for the protein matrix to modify the energetics of light harvesting. Such intricate pigment-protein interactions result in organized energy gradients and energy transfer pathways that are utilized to transfer excitation energy toward the RC, even in apparently irregular structures such as the FMO complex. In short, the protein scaffolding constructs a network of highly interconnected chlorophylls whose zeroth-order Hamiltonian, describing partially delocalized exciton states, already favors energy transfer toward the RC.

Emerging experimental data indicate that the dynamics of light harvesting is not fully described by a classical random-walk picture. Strong electronic couplings between spatially proximate chromophores give rise to delocalized exciton states and spatially connected EET pathways that are highly efficient. An intriguing addition to this picture is the quantum coherence effect, which can enable the excitation to rapidly and coherently sample multiple pathways in space. We suggest that such long-lasting excitonic coherence can be explained by the intrinsically small reorganization energy and potential for correlated bath motions in the protein environment inside PPCs. The fundamental issue of quantum coherence effects in natural biological systems demands more thorough theoretical and experimental investigations, perhaps using tools developed in quantum information science. The research can potentially open a revolutionary avenue for the effective use of biological systems as quantum devices or resources for quantum information processing.

SUMMARY POINTS

1. The nanoscale dimensions of light-harvesting PPCs result in strong couplings between pigments and energy tuning via pigment-protein interactions, which create energy transfer pathways that can channel energy flow efficiently toward the RC.
2. Based on structural information, site energies and excitonic couplings of excitations in a PPC can be determined using modern quantum chemical methods. However, including dielectric screening of the protein matrix and specific interactions between chromophores and protein residues is crucial for the accurate description of electronic excitations in photosynthetic PPCs.
3. Two-dimensional electronic spectroscopy is a particularly powerful tool for monitoring EET dynamics in photosynthetic PPCs because it is sensitive to electronic couplings and coherent dynamical processes in the system. Moreover, variants of 2D electronic spectroscopy can be developed to enhance specificity and resolution of 2D spectra.
4. Two energy transfer pathways control the energy flow in the FMO complex, and the energy transfer occurs via a wavelike, coherent mechanism, which can promote the efficiency of energy trapping in photosynthesis.
5. In natural light harvesting, coherence at an individual system level may be generated through the absorption of sunlight or EET from another light-harvesting complex, and the quantum effect can affect the outcome of energy trapping as long as the coherence within the system is maintained.

DISCLOSURE STATEMENT

The authors are not aware of any biases that might be perceived as affecting the objectivity of this review.

ACKNOWLEDGMENTS

G.R.F. thanks Prof. D.M. Jonas for valuable discussions. This work was supported by the Director, Office of Science, Office of Basic Energy Sciences, of the U.S. Department of Energy under contract DE-AC02-05CH11231 and by the Chemical Sciences, Geosciences and Biosciences Division, Office of Basic Energy Sciences, U.S. Department of Energy under contract DE-AC03-76SF000098.

LITERATURE CITED

1. van Amerongen H, Valkunas L, van Grondelle R. 2000. *Photosynthetic Excitons*. Singapore: World Sci.
2. Blankenship RE. 2002. *Molecular Mechanisms of Photosynthesis*. London: Blackwell Sci.
3. Duysens L. 1964. Photosynthesis. *Prog. Biophys. Mol. Biol.* 14:1–104
4. Sundström V, Pullerits T, van Grondelle R. 1999. Photosynthetic light-harvesting: Reconciling dynamics and structure of purple bacterial LH2 reveals function of photosynthetic unit. *J. Phys. Chem. B* 103:2327–46
5. Yang M, Agarwal R, Fleming GR. 2001. The mechanism of energy transfer in the antenna of photosynthetic purple bacteria. *J. Photochem. Photobiol. A* 142:107–19
6. **Hu X, Ritz T, Damjanovic A, Autenrieth F, Schulten K. 2002. Photosynthetic apparatus of purple bacteria. *Q. Rev. Biophys.* 35:1–62**

6. Comprehensive review of structure-based theoretical studies of EET dynamics in photosynthetic apparatus of purple bacteria.

7. Scholes GD, Fleming GR. 2005. Energy transfer and photosynthetic light harvesting. *Adv. Chem. Phys.* 132:57–130
8. van Grondelle R, Novoderezhkin VI. 2006. Energy transfer in photosynthesis: experimental insights and quantitative models. *Phys. Chem. Chem. Phys.* 8:793–807
9. Cogdell RJ, Gall A, Köhler J. 2006. The architecture and function of the light-harvesting apparatus of purple bacteria: from single molecules to in vivo membranes. *Q. Rev. Biophys.* 39:227–324
10. Sundström V. 2008. Femtobiology. *Annu. Rev. Phys. Chem.* 59:53–77
11. Sener MK, Jolley C, Ben-Shem A, Fromme P, Nelson N, et al. 2005. Comparison of the light-harvesting networks of plant and cyanobacterial photosystem I. *Biophys. J.* 89:1630–42
12. Vassiliev S, Bruce D. 2008. Toward understanding molecular mechanisms of light harvesting and charge separation in photosystem II. *Photosyn. Res.* 97:75–89
13. Cogdell RJ, Lindsay JG. 2000. The structure of photosynthetic complexes in bacteria and plants: an illustration of the importance of protein structure to the future development of plant science. *New Phytol.* 145:167–96
14. Fenna RE, Matthews BW, Olson JM, Shaw EK. 1974. Structure of a bacteriochlorophyll protein from the green photosynthetic bacterium *Chlorobium limicola*: crystallographic evidence for a trimer. *J. Mol. Biol.* 84:231–40
15. Li YF, Zhou W, Blankenship RE, Allen JP. 1997. Crystal structure of the bacteriochlorophyll a protein from *Chlorobium tepidum*. *J. Mol. Biol.* 271:456–71
16. Camara-Artigas A, Blankenship RE, Allen JP. 2003. The structure of the FMO protein from *Chlorobium tepidum* at 2.2 Å resolution. *Photosyn. Res.* 75:49–55
17. Matthews BW, Fenna RE, Bolognesi MC, Schmid MF, Olson JM. 1979. Structure of a bacteriochlorophyll a protein from the green photosynthetic bacterium *Prosthecochloris aestuarii*. *J. Mol. Biol.* 131:259–85
18. Tronrud DE, Schmid MF, Matthews BW. 1986. Structure and X-ray amino acid sequence of a bacteriochlorophyll a protein from *Prosthecochloris aestuarii* refined at 1.9 Å resolution. *J. Mol. Biol.* 188:443–54
19. Renger T, May V, Kuhn O. 2001. Ultrafast excitation energy transfer dynamics in photosynthetic pigment-protein complexes. *Phys. Rep.* 343:137–254
20. Förster T. 1948. Zwischenmolekulare Energiewanderung und Fluoreszenz. *Ann. Phys. (Berlin)* 437:55–75
21. Scholes GD. 2003. Long-range resonance energy transfer in molecular systems. *Annu. Rev. Phys. Chem.* 54:57–87
22. Alden RG, Johnson E, Nagarajan V, Parson W, Law C, et al. 1997. Calculations of spectroscopic properties of the LH2 bacteriochlorophyll-protein antenna complex from *Rhodopseudomonas acidophila*. *J. Phys. Chem. B* 101:4667–80
23. Cory M, Zerner M, Hu X, Schulten K. 1998. Electronic excitations in aggregates of bacteriochlorophylls. *J. Phys. Chem. B* 102:7640–50
24. Krueger BP, Scholes GD, Fleming GR. 1998. Calculation of couplings and energy-transfer pathways between the pigments of LH2 by the ab initio transition density cube method. *J. Phys. Chem. B* 102:5378–86
25. Scholes GD, Gould IR, Cogdell RJ, Fleming GR. 1999. Ab initio molecular orbital calculations of electronic couplings in the LH2 bacterial light-harvesting complex of *Rps. acidophila*. *J. Phys. Chem. B* 103:2543–53
26. Hsu CP, You ZQ, Chen HCH. 2008. Characterization of the short-range couplings in excitation energy transfer. *J. Phys. Chem. C* 112:1204–12
27. Jordanides X, Scholes GD, Fleming GR. 2001. The mechanism of energy transfer in the bacterial photosynthetic reaction center. *J. Phys. Chem. B* 105:1652–69
28. Jordanides X, Scholes GD, Shapley W, Reimers JR, Fleming GR. 2004. Electronic couplings and energy transfer dynamics in the oxidized primary electron donor of the bacterial reaction center. *J. Phys. Chem. B* 108:1753–65
29. Madjet MEA, Abdurahman A, Renger T. 2006. Intermolecular Coulomb couplings from ab initio electrostatic potentials: application to optical transitions of strongly coupled pigments in photosynthetic antennae and reaction centers. *J. Phys. Chem. B* 110:17268–81

8. Clear and current review of experimental and theoretical studies of energy transfer in the photosynthetic light-harvesting complexes LH1, LH2, and LHCII.

19. In-depth review of the theoretical modeling of optical properties and EET dynamics in photosynthetic PPCs.

21. Summarizes the various approximations in Förster theory and the development of a more general theoretical description of resonance energy transfer in donor-acceptor pairs.

30. Adolphs J, Renger T. 2006. How proteins trigger excitation energy transfer in the FMO complex of green sulfur bacteria. *Biophys. J.* 91:2778–97
31. Louwe R, Vrieze J, Hoff A, Aartsma TJ. 1997. Toward an integral interpretation of the optical steady-state spectra of the FMO complex of *Prosthecochloris aestuarii*. 2. Exciton simulations. *J. Phys. Chem. B* 101:11280–87
32. Hsu C, Fleming GR, Head-Gordon M, Head-Gordon T. 2001. Excitation energy transfer in condensed media. *J. Chem. Phys.* 114:3065–72
33. Iozzi MF, Mennucci B, Tomasi J, Cammi R. 2004. Excitation energy transfer (EET) between molecules in condensed matter: a novel application of the polarizable continuum model (PCM). *J. Chem. Phys.* 120:7029–40
34. Curutchet C, Mennucci B. 2005. Toward a molecular scale interpretation of excitation energy transfer in solvated bichromophoric systems. *J. Am. Chem. Soc.* 127:16733–44
35. Scholes GD, Curutchet C, Mennucci B, Cammi R, Tomasi J. 2007. How solvent controls electronic energy transfer and light harvesting. *J. Phys. Chem. B* 111:6978–82
36. Curutchet C, Scholes GD, Mennucci B, Cammi R. 2007. How solvent controls electronic energy transfer and light harvesting: toward a quantum-mechanical description of reaction field and screening effects. *J. Phys. Chem. B* 111:13253–65
37. Fowler GJ, Visschers RW, Grief GG, van Grondelle R, Hunter CN. 1992. Genetically modified photosynthetic antenna complexes with blueshifted absorbance bands. *Nature* 355:848–50
38. Fowler GJ, Sockalingum GD, Robert B, Hunter CN. 1994. Blue shifts in bacteriochlorophyll absorbance correlate with changed hydrogen bonding patterns in light-harvesting 2 mutants of *Rhodobacter sphaeroides* with alterations at α-Tyr-44 and α-Tyr-45. *Biochem. J.* 299:695–700
39. Müh F, Madjet MEA, Adolphs J, Abdurahman A, Rabenstein B, et al. 2007. α-Helices direct excitation energy flow in the Fenna Matthews Olson protein. *Proc. Natl. Acad. Sci. USA* 104:16862–67
40. Adolphs J, Müh F, Madjet MEA, Renger T. 2008. Calculation of pigment transition energies in the FMO protein: from simplicity to complexity and back. *Photosyn. Res.* 95:197–209
41. Breuer HP, Petruccione F. 2002. *The Theory of Open Quantum Systems*. Oxford: Oxford Univ. Press
42. Yang M, Fleming GR. 2002. Influence of phonons on exciton transfer dynamics: comparison of the Redfield, Förster, and modified Redfield equations. *Chem. Phys.* 282:163–80
43. Fleming GR, Cho M. 1996. Chromophore-solvent dynamics. *Annu. Rev. Phys. Chem.* 47:109–34
44. Mukamel S. 1995. *Principles of Nonlinear Optical Spectroscopy*. Oxford: Oxford Univ. Press
45. Scholes GD, Fleming GR. 2000. On the mechanism of light harvesting in photosynthetic purple bacteria: B800 to B850 energy transfer. *J. Phys. Chem. B* 104:1854–68
46. Scholes GD, Jordanides X, Fleming GR. 2001. Adapting the Förster theory of energy transfer for modeling dynamics in aggregated molecular assemblies. *J. Phys. Chem. B* 105:1640–51
47. Sumi H. 1999. Theory on rates of excitation energy transfer between molecular aggregates through distributed transition dipoles with application to the antenna system in bacterial photosynthesis. *J. Phys. Chem. B* 103:252–60
48. Sumi H. 2002. Bacterial photosynthesis begins with quantum-mechanical coherence. *Chem. Rec.* 1:480–93
49. Jang S, Newton MD, Silbey RJ. 2004. Multichromophoric Förster resonance energy transfer. *Phys. Rev. Lett.* 92:218301
50. Jang S, Jung Y, Silbey RJ. 2002. Nonequilibrium generalization of Förster-Dexter theory for excitation energy transfer. *Chem. Phys.* 275:319–32
51. Jang S. 2007. Generalization of the Förster resonance energy transfer theory for quantum mechanical modulation of the donor-acceptor coupling. *J. Chem. Phys.* 127:174710
52. Cheng YC, Silbey RJ. 2006. Coherence in the B800 ring of purple bacteria LH2. *Phys. Rev. Lett.* 96:028103
53. Jang S, Newton MD, Silbey RJ. 2007. Multichromophoric Förster resonance energy transfer from b800 to b850 in the light harvesting complex 2: evidence for subtle energetic optimization by purple bacteria. *J. Phys. Chem. B* 111:6807–14
54. Redfield AG. 1957. On the theory of relaxation processes. *IBM J. Res. Dev.* 1:19–31
55. Suarez A, Silbey RJ, Oppenheim I. 1992. Memory effects in the relaxation of quantum open systems. *J. Chem. Phys.* 97:5101–7

39. Calculates the site energies of the seven BChls in the FMO complex including molecular details of the protein environment, based only on the structural information.

42. Explains the limitations and domains of applicability of the Redfield, Förster, and modified-Redfield equations.

48. Along with Reference 49, generalizes the Förster approach to treat multichromophoric effects arising from the coherence within donor or acceptor groups.

56. Cheng YC, Silbey RJ. 2005. Markovian approximation in the relaxation of open quantum systems. *J. Phys. Chem. B* 109:21399–405
57. Cho M, Vaswani HM, Brixner T, Stenger J, Fleming GR. 2005. Exciton analysis in 2D electronic spectroscopy. *J. Phys. Chem. B* 109:10542–56
58. Ohtsuki Y, Fujimura Y. 1996. Theoretical study of bath-induced coherence transfer effects on a time- and frequency-resolved resonant light scattering spectrum. 2. Energy mismatch effects. *J. Chem. Phys.* 104:8321–31
59. Ohtsuki Y, Fujimura Y. 1989. Bath-induced vibronic coherence transfer effects on femtosecond time-resolved resonant light scattering spectra from molecules. *J. Chem. Phys.* 91:3903–15
60. Kuhn O, Sundström V, Pullerits T. 2002. Fluorescence depolarization dynamics in the B850 complex of purple bacteria. *Chem. Phys.* 275:15–30
61. Novoderezhkin VI, Wendling M, van Grondelle R. 2003. Intra- and interband transfers in the B800–B850 antenna of *Rhodospirillum molischianum*: Redfield theory modeling of polarized pump-probe kinetics. *J. Phys. Chem. B* 107:11534–48

62. Engel GS, Calhoun TR, Read EL, Ahn TK, Mancal T, et al. 2007. Evidence for wavelike energy transfer through quantum coherence in photosynthetic systems. *Nature* 446:782–86

62. Observes long-lasting excitonic coherence and coherent energy transfer in the FMO complex.

63. Jean J, Fleming GR. 1995. Competition between energy and phase relaxation in electronic curve crossing processes. *J. Chem. Phys.* 103:2092–101
64. Khalil M, Demirdoven N, Tokmakoff A. 2004. Vibrational coherence transfer characterized with Fourier-transform 2D IR spectroscopy. *J. Chem. Phys.* 121:362–73
65. Kenkre VM, Knox RS. 1974. Generalized-master-equation theory of excitation transfer. *Phys. Rev. B* 9:5279–90
66. Silbey R. 1976. Electronic energy transfer in molecular crystals. *Annu. Rev. Phys. Chem.* 27:203–23
67. Munn R, Silbey RJ. 1980. Remarks on exciton-phonon coupling and exciton transport. *Mol. Cryst. Liq. Cryst.* 57:131–44
68. Novoderezhkin VI, Palacios MA, van Amerongen H, van Grondelle R. 2004. Energy-transfer dynamics in the LHCII complex of higher plants: modified Redfield approach. *J. Phys. Chem. B* 108:10363–75
69. Novoderezhkin VI, Rutkauskas D, van Grondelle R. 2006. Dynamics of the emission spectrum of a single LH2 complex: interplay of slow and fast nuclear motions. *Biophys. J.* 90:2890–902
70. Schröder M, Kleinekathöfer U, Schreiber M. 2006. Calculation of absorption spectra for light-harvesting systems using non-Markovian approaches as well as modified Redfield theory. *J. Chem. Phys.* 124:084903
71. Renger T, Trostmann I, Theiss C, Madjet MEA, Richter M, et al. 2007. Refinement of a structural model of a pigment-protein complex by accurate optical line shape theory and experiments. *J. Phys. Chem. B* 111:10487–501
72. Zhang W, Meier T, Chernyak V, Mukamel S. 1998. Exciton-migration and three-pulse femtosecond optical spectroscopies of photosynthetic antenna complexes. *J. Chem. Phys.* 108:7763–74
73. Golosov AA, Reichman DR. 2001. Reference system master equation approaches to condensed phase charge transfer processes. I. General formulation. *J. Chem. Phys.* 115:9848–61
74. Golosov AA, Reichman DR. 2001. Reference system master equation approaches to condensed phase charge transfer processes. II. Numerical tests and applications to the study of photoinduced charge transfer reactions. *J. Chem. Phys.* 115:9862–70

75. Lee H, Cheng YC, Fleming GR. 2007. Coherence dynamics in photosynthesis: protein protection of excitonic coherence. *Science* 316:1462–65

75. Observes long-lasting coherence in a bacterial RC and shows that this phenomenon is explained by a correlated protein environment.

76. Mukamel S. 2000. Multidimensional femtosecond correlation spectroscopies of electronic and vibrational excitations. *Annu. Rev. Phys. Chem.* 51:691–729
77. Jonas DM. 2003. Two-dimensional femtosecond spectroscopy. *Annu. Rev. Phys. Chem.* 54:425–63
78. Cho M. 2008. Coherent two-dimensional optical spectroscopy. *Chem. Rev.* 108:1331–418

79. Cho M, Brixner T, Stiopkin IV, Vaswani HM, Fleming GR. 2006. Two dimensional electronic spectroscopy of molecular complexes. *J. Chin. Chem. Soc.* 53:15–24

79. Provides an intuitive description of the origin and information content of 2D electronic spectra.

80. Cheng YC, Engel GS, Fleming GR. 2007. Elucidation of population and coherence dynamics using cross-peaks in two-dimensional electronic spectroscopy. *Chem. Phys.* 341:285–95
81. Hybl J, Yu A, Farrow D, Jonas DM. 2002. Polar solvation dynamics in the femtosecond evolution of two-dimensional Fourier transform spectra. *J. Phys. Chem. A* 106:7651–54

82. Stiopkin IV, Brixner T, Yang M, Fleming GR. 2006. Heterogeneous exciton dynamics revealed by two-dimensional optical spectroscopy. *J. Phys. Chem. B* 110:20032–37
83. Roberts ST, Loparo JJ, Tokmakoff A. 2006. Characterization of spectral diffusion from two-dimensional line shapes. *J. Chem. Phys.* 125:084502
84. Pisliakov AV, Mancal T, Fleming GR. 2006. Two-dimensional optical three-pulse photon echo spectroscopy. II. Signatures of coherent electronic motion and exciton population transfer in dimer two-dimensional spectra. *J. Chem. Phys.* 124:234505
85. Cho M, Fleming GR. 2005. The integrated photon echo and solvation dynamics. II. Peak shifts and two-dimensional photon echo of a coupled chromophore system. *J. Chem. Phys.* 123:114506
86. Cheng YC, Fleming GR. 2008. Coherence quantum beats in two-dimensional electronic spectroscopy. *J. Phys. Chem. A* 112:4254–60
87. Hybl J, Christophe Y, Jonas DM. 2001. Peak shapes in femtosecond 2D correlation spectroscopy. *Chem. Phys.* 266:295–309
88. Khalil M, Demirdoven N, Tokmakoff A. 2003. Coherent 2D IR spectroscopy: molecular structure and dynamics in solution. *J. Phys. Chem. A* 107:5258–79
89. Zigmantas D, Read EL, Mancal T, Brixner T, Gardiner AT, et al. 2006. Two-dimensional electronic spectroscopy of the B800–B820 light-harvesting complex. *Proc. Natl. Acad. Sci. USA* 103:12672–77
90. Hochstrasser RM. 2001. Two-dimensional IR spectroscopy: polarization anisotropy effects. *Chem. Phys.* 266:273–84
91. Zanni MT, Ge NH, Kim YS, Hochstrasser RM. 2001. Two-dimensional IR spectroscopy can be designed to eliminate the diagonal peaks and expose only the crosspeaks needed for structure determination. *Proc. Natl. Acad. Sci. USA* 98:11265–70
92. Dreyer J, Moran A, Mukamel S. 2003. Tensor components in three pulse vibrational echoes of a rigid dipeptide. *Bull. Kor. Chem. Soc.* 24:1091–96
93. Read EL, Engel GS, Calhoun TR, Mancal T, Ahn TK, et al. 2007. Cross-peak-specific two-dimensional electronic spectroscopy. *Proc. Natl. Acad. Sci. USA* 104:14203–8
94. Voronine DV, Abramavicius D, Mukamel S. 2007. Manipulating multidimensional electronic spectra of excitons by polarization pulse shaping. *J. Chem. Phys.* 126:044508
95. Abramavicius D, Mukamel S. 2006. Chirality-induced signals in coherent multidimensional spectroscopy of excitons. *J. Chem. Phys.* 124:034113
96. Voronine DV, Abramavicius D, Mukamel S. 2006. Coherent control of cross-peaks in chirality-induced two-dimensional optical signals of excitons. *J. Chem. Phys.* 125:224504
97. Abramavicius D, Voronine DV, Mukamel S. 2008. Unravelling coherent dynamics and energy dissipation in photosynthetic complexes by 2D spectroscopy. *Biophys. J.* 94:3613–19
98. Read E, Schlau-Cohen G, Engel GS, Wen J, Blankenship RE, et al. 2008. Visualization of excitonic structure in the Fenna-Matthews-Olson photosynthetic complex by polarization-dependent two-dimensional electronic spectroscopy. *Biophys. J.* 95:847–56
99. Vulto SIE, Neerken S, Louwe R, de Baat M, Amesz J, et al. 1998. Excited-state structure and dynamics in FMO antenna complexes from photosynthetic green sulfur bacteria. *J. Phys. Chem. B* 102:10630–35
100. Vulto SIE, de Baat M, Louwe R, Permentier HP, Neef T, et al. 1998. Exciton simulations of optical spectra of the FMO complex from the green sulfur bacterium *Chlorobium tepidum* at 6 K. *J. Phys. Chem. B* 102:9577–82
101. Wendling M, Przyjalgowski MA, Gülen D, Vulto SIE, Aartsma TJ, et al. 2005. The quantitative relationship between structure and polarized spectroscopy in the FMO complex of *Prosthecochloris aestuarii*: refining experiments and simulations. *Photosyn. Res.* 71:99–123
102. Freiberg A, Lin S, Timpmann K, Blankenship RE. 1997. Exciton dynamics in FMO bacteriochlorophyll protein at low temperatures. *J. Phys. Chem. B* 101:7211–20
103. Savikhin S, Buck DR, Struve WS. 1998. Toward level-to-level energy transfers in photosynthesis: the Fenna-Matthews-Olson protein. *J. Phys. Chem. B* 102:5556–65
104. Brixner T, Stenger J, Vaswani HM, Cho M, Blankenship RE, et al. 2005. Two-dimensional spectroscopy of electronic couplings in photosynthesis. *Nature* 434:625–28
105. Yang M, Fleming GR. 1999. Two-color three-pulse photon echoes as a probe of electronic coupling in molecular complexes. *J. Chem. Phys.* 110:2983–90

104. First 2D electronic spectroscopic experiment on a photosynthetic complex, showing the EET pathways in the FMO complex.

106. Mancal T, Fleming GR. 2004. Probing electronic coupling in excitonically coupled heterodimer complexes by two-color three-pulse photon echoes. *J. Chem. Phys.* 121:10556–65
107. Parkinson DY, Lee H, Fleming GR. 2007. Measuring electronic coupling in the reaction center of purple photosynthetic bacteria by two-color, three-pulse photon echo peak shift spectroscopy. *J. Phys. Chem. B* 111:7449–56
108. Cheng YC, Lee H, Fleming GR. 2007. Efficient simulation of three-pulse photon-echo signals with application to the determination of electronic coupling in a bacterial photosynthetic reaction center. *J. Phys. Chem. A* 111:9499–508
109. Wen J, Zhang H, Gross ML, Blankenship RE. 2008. Membrane orientation of the FMO antenna protein from *Chlorobium tepidum* as determined by mass spectrometry-based footprinting. Unpublished manuscript
110. Robinson GW. 1966. Excitation transfer and trapping in photosynthesis. In *Brookhaven Symposium in Biology, No. 19*, pp. 16–48. Upton, NY: Brookhaven Natl. Lab.
111. Pearlstein RM. 1982. Exciton migration and trapping in photosynthesis. *Photochem. Photobiol.* 35:835–44
112. Leegwater J. 1996. Coherent versus incoherent energy transfer and trapping in photosynthetic antenna complexes. *J. Phys. Chem.* 100:14403–9
113. Monshouwer R, Abrahamsson M, van Mourik F, van Grondelle R. 1997. Superradiance and exciton delocalization in bacterial photosynthetic light-harvesting systems. *J. Phys. Chem. B* 101:7241–48
114. Chachisvilis M, Kuhn O, Pullerits T, Sundström V. 1997. Excitons in photosynthetic purple bacteria: wavelike motion or incoherent hopping? *J. Phys. Chem. B* 101:7275–83
115. Meier T, Chernyak V, Mukamel S. 1997. Multiple exciton coherence sizes in photosynthetic antenna complexes viewed by pump-probe spectroscopy. *J. Phys. Chem. B* 101:7332–42
116. Savikhin S, Buck DR, Struve WS. 1997. Oscillating anisotropies in a bacteriochlorophyll protein: evidence for quantum beating between exciton levels. *Chem. Phys.* 223:303–12
117. Jean J. 1996. Vibrational coherence effects on electronic curve crossing. *J. Chem. Phys.* 104:5638–46
118. Calhoun T, Schlau-Cohen G, Ginsberg N, Fleming GR. 2008. Unpublished manuscript
119. Gaab KM, Bardeen CJ. 2004. The effects of connectivity, coherence, and trapping on energy transfer in simple light-harvesting systems studied using the Haken-Strobl model with diagonal disorder. *J. Chem. Phys.* 121:7813–20
120. Gouy M. 1886. Sur le mouvement lumineux. *J. Phys. Theor. Appl.* 5:354–62
121. Rayleigh J. 1889. On the character of the complete radiation at a given temperature. *Philos. Mag.* 27:460–69
122. Bradley D, New G. 1974. Ultrashort pulse measurements. *Proc. IEEE* 62:313–45
123. Hwang H, Rossky PJ. 2004. An analysis of electronic dephasing in the spin-boson model. *J. Chem. Phys.* 120:11380–85

Annual Review of
Physical Chemistry

Volume 60, 2009

Contents

Indexes

Errata

An online log of corrections to *Annual Review of Physical Chemistry* articles may be found at http://physchem.annualreviews.org/errata.shtml